Available online at www.sciencedirect.com
SCIENCE DIRECT®
Journal of Chromatography A, 1034 (2004) 85–97
JOURNAL OF CHROMATOGRAPHY A
www.elsevier.com/locate/chroma

# Comparison of chromatographic ion-exchange resins III. Strong cation-exchange resins

Arne Staby [a,*], Maj-Britt Sand [b], Ronni G. Hansen [c], Jan H. Jacobsen [d], Line A. Andersen [e], Michael Gerstenberg [e], Ulla K. Bruus [a], Inge Holm Jensen [a]

[a] *Novo Nordisk A/S, Protein Separation, Hagedornsvej 1, DK-2820 Gentofte, Denmark*
[b] *Protein Chemistry, Gentofte, Denmark*
[c] *Diabetes Bulk Production, Kalundborg, Denmark*
[d] *QA Fermentation & Recovery, Kalundborg, Denmark*
[e] *Novo Nordisk A/S, Sensor Technologies, Brennum Park, DK-3400 Hillerød, Denmark*

Received 1 August 2003; received in revised form 15 January 2004; accepted 16 January 2004

**Abstract**

A comparative study was performed on strong cation-exchangers to investigate the pH dependence, efficiency, binding strength, particle size distribution, static and dynamic capacity, and SEM pictures of chromatographic resins. The resins tested included: SP Sepharose XL, Poros 50 HS, Toyopearl SP 550c, SP Sepharose BB, Source 30S, TSKGel SP-5PW-HR20, and Toyopearl SP 650c. Testing was performed with four different proteins: anti-FVII Mab (IgG), aprotinin, lysozyme, and myoglobin. Dependence of pH on retention was generally very low for proteins with high pI. An unexpected binding at pH 7.5 of anti-FVII Mab with pI $< 7.5$ was observed on several resins. Efficiency results show the expected trend of higher dependence of the plate height with increasing flow rate of soft resins compared to resins for medium and high-pressure operation. Determination of particle size distribution by two independent methods, Coulter counting and SEM, was in very good agreement. The mono-dispersed nature of Source 30S was confirmed. Binding to cation-exchange resins as a function of ionic strength varies depending on the specific protein. Generally, binding and elution at high salt concentration may be performed with Toyopearl SP 550c and Poros 50 HS, while binding and elution at low salt concentration may be performed with Toyopearl SP 650c. A very high binding capacity was obtained with SP Sepharose XL. Comparison of static capacity and dynamic capacity at 10% break-through shows in general approximately 50–80% utilisation of the total available capacity during chromatographic operation. A general good agreement was obtained between this study and data obtained by others. The results of this study may be used for selection of resins for testing in process development. The validity of experiments and results with model proteins were tested using human insulin precursor in pure state and in real feed-stock on Toyopearl SP 550c, SP Sepharose BB, and Toyopearl SP 650c. Results showed good agreement with experiments with model proteins.


*Keywords:* Static capacity; Dynamic capacity; Stationary phases, LC; Ion-exchangers; Proteins

## 1. Introduction

Ion-exchange chromatography of proteins and peptides for preparative separation has been a standard technique for many years in the pharmaceutical industry. The popularity of this technique is due to the simple methodology and to the preservation of biological activity of the proteins and peptides during the ion-exchange processing. Comparison of chromatographic resins is performed during process development, but due to time constraints only a limited number of resins is regularly tested for the specific application. Results of such resin comparisons are hardly ever published unless very surprising or patentable discoveries are made.

A number of papers comparing cation-exchangers has been published by commercial suppliers and non-commercial authors [1–24] comparing various parameters including: dynamic [2,5–7,9,15,16,19,22,23], static [2,3,6,11,16,23], and ionic [2–6,11,22] capacities, binding strength [4,10,15,17–20,22], elution dependence on pH [8,10,14,15,17,18], efficiency [6,9,10,12,14,17,22,23], resolution [2,3,5–7,11,14,15,17,19–24], adsorption isotherms [6,13,16,18], pressure drop [5,6,11,14,17,23], compressibility [3,5,6,14], protein

* Corresponding author. Tel.: +45-44439989; fax: +45-44438400.

0021-9673/$ – see front matter © 2004 Elsevier B.V. All rights reserved.
doi:10.1016/j.chroma.2004.01.026

recovery [3,5,6,14,17], operating flow rate [3,5,6,9], cost etc. [5,24], chemical stability [5,11,14,17], base matrix chemistry [2,4,11,13,14,17,23,24], pore size distribution [1,4,9,17], and others. The number of resins compared in these papers is typically two to four, however, the papers of DePhillips and Lenhoff [1,4], Boschetti [2], Levison et al. [3], Noel and Proctor [5], Nash and Chase [6], and Chang and Lenhoff [13], include more than four cation-exchangers. The test proteins used are typically lysozyme, chymotrypsinogen, cytochrome C, IgG and others.

This work is part of a continuing study performed at Novo Nordisk to characterise and compare old and new commercial ion-exchangers for improved selection for testing in process development. We have previously published the results of 17 strong anion-exchange resins comparing dynamic capacities, titration curves, binding strength, elution dependence on pH, and efficiency by a systematic and consistent experimental setup [25,26]. The scope of this paper is to compare seven commercial, strong cation-exchangers, that is, resins with ligates containing a sulphonic acid group. The comparison include data on efficiency, binding strength, pH dependence, particle size distribution, dynamic and static capacity, and SEM pictures of the cation-exchange resins performed at the same, relevant conditions. The four test proteins used cover a broad range of isoelectric points and molecular weights. They include both standard test proteins (lysozyme and myoglobin) and a protein and a peptide obtained at Novo Nordisk (anti-FVII Mab (IgG) [27] and aprotinin [28]). The validity of model experiments and results was tested using a protein, human insulin precursor from Novo Nordisk [31], in pure state and in real feed-stock. The study represents approximately 1100 experimental measurements.

## 2. Experimental

### 2.1. Materials

SP Sepharose XL, SP Sepharose Big Beads, and Source 30S beads were kindly donated by Amersham Biosciences (Uppsala, Sweden). Poros 50 HS beads were kindly donated by PE Biosystems (Cambridge, MA, USA). Toyopearl SP 550c, Toyopearl SP 650c, and TSKGel SP-5PW-HR20 beads were kindly donated by TOSOH BIOSEP (Stuttgart, Germany).

Chicken egg white lysozyme (L6876) and horse skeletal muscle myoglobin (M0630) were purchased from Sigma (St. Louis, MO, USA). The industrial proteins/peptides in pure state and in real feed-stock (anti-FVII Mab, aprotinin, and insulin precursor) were obtained from Novo Nordisk A/S (Bagsværd, Denmark).

2-(*N*-Morpholino)-ethanesulphonic acid (MES, M8250) and *N*-(2-Hydroxyethyl)-piperazine-*N*′-(2-ethanesulphonic acid) (HEPES, H3375) were purchased from Sigma Chemical Co. (St. Louis, MO, USA). Sodium acetate (1.06267) and the other chemicals: sodium chloride, hydrochloric acid, and acetone were analytical reagent grade and purchased from Merck (Darmstadt, Germany).

### 2.2. Instrumentation

A BioCAD Workstation from PE Biosystems (Cambridge, MA, USA) was used for chromatographic measurements and evaluation in these studies. The standard BioCAD Workstation was equipped with a 100 μl sample injection loop, a 0.6 cm flow cell, pump heads for flow rates between 0.2 and 60 ml/min, and mixing of standard buffer solutions (standard BioCAD buffer setup) was obtained through a mixing valve. UV detection was operated at 280 nm. The BioCAD was placed in a temperature controlled airbath from Brønnum (Herlev, Denmark) to maintain a constant temperature of 22 ± 1 °C throughout the measurements. UV-Vis spectrophotometry for sample concentration adjustment was carried out on a HP8452A (Birkerød, Denmark).

Source 30S was packed at medium pressure in a 10 cm length × 0.46 cm i.d. OmegaChrom PEEK column from Upchurch (Oak Harbor, WA, USA). Other chromatographic resins were packed in HR 5/10 columns (10 cm length × 0.5 cm i.d.) supplied by Amersham Biosciences (Uppsala, Sweden).

Measurement of optical density at 280 nm ($OD_{280}$) for static capacity determination was performed using a diode array spectrophotometer 8452A from Hewlett-Packard (Palo Alto, CA, USA).

Coulter counting for particle size distribution measurement was performed using a Coulter multisizer and sampling stand model S ST II from Coulter Electronics (Luton, UK).

Scanning electron microscopy (SEM) was carried out using a FEI Quanta 200 scanning electron microscope from FEI Company (Hillsboro, USA).

### 2.3. Methods

The methods used in this study are equal to those of our previous experiments [25,26]. The resin comparison experiments were performed employing similar conditions, that is, the same scale, buffers, buffer concentration, temperature, protein concentration, solution conductivity, pH, gradients, and corresponding flow rates, where appropriate. Experiments were made in duplicate. The pH of buffer and protein/peptide solutions was adjusted with hydrochloric acid or sodium hydroxide. The following general methodology was used.

The column was equilibrated with a sufficient number of column volumes (CVs) of buffer (15–20 CVs). Samples of 1 mg/ml pure protein solutions were applied through the injection system or in case of frontal analysis experiments through the pump. Lysozyme and myoglobin freeze-dried products were dissolved directly in equilibration buffer pH 5.5 for frontal analysis experiments and in water for other experiments. Freeze-dried aprotinin was dissolved in water

Table 1
Properties of test proteins

| Protein | pI | Molecular weight (kDa) |
|---|---|---|
| Anti-FVII Mab (IgG) | ~ 6–7 | 150 |
| Aprotinin | ~ 10.5 | 6 |
| Lysozyme | ~ 11 | 14 |
| Myoglobin | 7–8 | 18 |
| Insulin precursor | 5.3 | 6 |

pH 5.5 for all experiments. Anti-FVII Mab was obtained at a concentration of 2 mg/ml in a 50 mM Tris + 100 mM NaCl, pH 8.0 solution, which was diluted with one volume of water and adjusted to pH 5.5 for all experiments. Properties of the test proteins are given in Table 1. In all experiments a standard buffer solution concentration of 16.7 mM MES + 16.7 mM HEPES + 16.7 mM sodium acetate was used. Column regeneration was performed with 5 CVs of 1.0 M NaCl in binding strength and frontal analysis experiments.

Packing of columns was performed according to manufacturer specifications. Properties of the anion-exchange resins and flow rates applied in these studies are presented in Table 2. Recommended maximum operating pressure/flow rate were obtained from the suppliers. The general flow rate used for pH dependence and binding strength measurements was approximately 50% of the recommended maximum operating flow rate/pressure. The low and high flow rates used for dynamic capacity determinations were approximately 25 and 75%, respectively, of the recommended maximum operating flow rate/pressure.

Extra column volume measurements of the system were performed as described elsewhere [25].

### 2.3.1. pH dependence measurements

pH dependence measurements were performed at pH 4.5, 5.5, 6.5, and 7.5. Sample injection was done after column equilibration followed by a NaCl gradient from 0 to 1 M during 20 CVs. A small isocratic segment corresponding to the dead volume from the pump mixing system to the injection system was part of the method. The pH dependence experiments were in most cases performed with all four test proteins.

Retention factors, $k'$, for the gradient runs were defined and calculated based on the retention time of the peaks:

$$k' = \frac{t_R - M_{1,0}}{M_{1,0} - M_{1,S}}$$

where $t_R$ is the retention time of the protein, $M_{1,S}$ is the first moment of the extra column volume, and $M_{1,0}$ is the first moment of the protein at non-binding conditions found from the plate height determinations below.

### 2.3.2. Efficiency determinations

Efficiency determinations were performed as plate height determinations at the non-binding isocratic, conditions of 1 M NaCl, pH 7.5 as a function of flow rate. Flow rates were varied between approximately 10 and 100% of the recommended maximum flow rate/pressure. The experiments were in most cases performed with all four test proteins.

To get the best representation of the plate height, the peaks were fitted to an EMG function (exponentially modified Gaussian function) using the software programme TableCurve 2D ver. 2.03 from Jandel Scientific (San Rafael, CA, USA). The first and second moments were used to calculate the reduced plate height, $h$. The EMG function for fitting of raw data was chosen because of the somewhat tailing peaks obtained by efficiency measurements at non-binding conditions and especially by isocratic retention measurements at binding conditions, see below. The EMG function has the advantage of using the entire peak curve for the fit compared to the various graphical methods used for fitting to a Gaussian peak. The EMG function used is a five parameter model:

$$f(t) = \frac{A\sigma}{\tau\sqrt{2}} \exp\left[\left(\frac{\sigma}{\tau}\right)^2 \frac{1}{2} - \frac{t-\mu}{\tau}\right] \int_{-\infty}^{Z} e^{-x^2}\,dx + E,$$

$$\text{with } Z = \frac{1}{\sqrt{2}}\left(\frac{t-\mu}{\sigma} - \frac{\sigma}{\tau}\right)$$

where $t$ is the time, $A$ the scaling, $\mu$ the Gaussian mean value, $\sigma$ the symmetrical peak width, $\tau$ the asymmetrical

Table 2
Properties of the chromatographic cation-exchange resins and applied flow rates

| Resin | Particle size (μm) (supplier data) | Mean particle size (μm) (Coulter counting) | Mean particle size (μm) (SEM) | Maximum recommended pressure (bar) | Applied flow rates (ml/min) | | |
|---|---|---|---|---|---|---|---|
| | | | | | General | Capacity (low) | Capacity (high) |
| SP Sepharose XL | 90 (45–165) | 66 | 52 (32–87) | 3 | 1.2 | 0.6 | 1.8 |
| SP Sepharose BB | 200 (100–300) | 99 | 98 (65–196) | 3 | 1.2 | 0.6 | 1.8 |
| Poros 50 HS | 50 | 44 | 49 (19–67) | 100 | 4.0 | 2.0 | 10.0 |
| Source 30S | 30 | 27 | 31 (30–32) | 10–20 | 3.0 | 1.0 | 3.0 |
| Toyopearl SP 550c | 100 (50–150) | 80 | 78 (46–135) | 5 | 1.0 | 0.5 | 1.7 |
| Toyopearl SP 650c | 100 (50–150) | 80 | 93 (58–142) | 5 | 1.0 | 0.5 | 1.7 |
| TSKGel SP-5PW-HR20 | 20 (15–25) | 22 | 22 (16–26) | 20 | 2.5 | 1.0 | 3.0 |

General flow rate is used for pH dependence, binding strength measurements, while Capacity low and high flow rates are used for dynamic capacity determinations. Mean particle size is found from Coulter counting experiments and SEM pictures.

peak width, and $E$ the peak base line level. Fits to the EMG function were generally performed with a correlation factor higher than 0.99, and in most cases higher than 0.999. In a few difficult cases, fits to the EMG function were performed with a correlation factor down to 0.90. The first and second moments, $M_1$ and $M_2$, of the peak curve [29]:

$$M_1 = \mu + \tau$$

$$M_2 = \sigma^2 + \tau^2$$

are additive parameters, thus for an exponentially modified Gaussian peak the reduced theoretical plate height of the column, $h$, is found from:

$$h = \frac{H}{d_p} = \frac{L}{d_p N} = \frac{L(M_{2,0} - M_{2,S})}{d_p(M_{1,0} - M_{1,S})^2}$$

where $H$ is the theoretical plate height, $d_p$ the particle diameter, $L$ the column length, $N$ the number of theoretical plates of the column, $M_{2,0}$ the second moment of the protein peak at non-binding conditions, and $M_{2,S}$ the second moment of the extra column volume. $h$ is in this study presented as a function of the linear flow rate, $v$:

$$v = \frac{v_{vol}}{\pi r^2}$$

where $v_{vol}$ is the volumetric flow rate and $r$ the column radius.

#### 2.3.3. Binding strength measurements

Binding strength experiments were performed as the classical isocratic retention measurements as a function of NaCl concentration, which was varied between 0 and 550 mM depending on the resin and the protein. For all proteins, the binding strength experiments were performed at pH 5.5.

The best representation of data was achieved by fitting the peaks to an EMG function. The first moment of the fit was used to calculate the retention factor, $k'$:

$$k' = \frac{M_1 - M_{1,0}}{M_{1,0} - M_{1,S}}$$

using the first moments of the extra column volume and the efficiency data at non-binding conditions for adjustment. The binding strength is illustrated by plotting $k'$ versus reciprocal total ionic strength of the solution for elution. The total ionic strength, $I_{Total}$, was found from:

$$I_{Total} = 0.5 \sum_i c_i {z_i}^2$$

where $c_i$ is the molar concentration and $z_i$ the ionic charge of the ionic species $i$ in the solution for elution.

#### 2.3.4. Dynamic capacity determinations

Dynamic capacity was determined by frontal analysis experiments with anti-FVII Mab, aprotinin, and lysozyme. The column was equilibrated with 15 CVs of the standard buffer solution (16.7 mM MES + 16.7 mM HEPES + 16.7 mM sodium acetate) without salt at pH 5.5. Other conditions were performed according to the method described elsewhere [25]. Based on the UV signals obtained, the level of break-through was calculated by normalising the protein concentration with the initial protein concentration, $C/C_0$. The dynamic capacity at 10 and 50% break-through is presented in this study.

#### 2.3.5. Static capacity determinations

Static capacity was determined by batch adsorption experiments with anti-FVII Mab, aprotinin, and lysozyme. Resins were packed and equilibrated as stated previously with buffer solution at pH 5.5. $OD_{280}$ of a 1 mg/ml protein solution was measured. Resins were poured out of the column into a beaker containing the protein solution. Based on results from dynamic capacity experiments, the total amount of protein in solution was two times that found per ml of resin. Solutions were left standing overnight (16–20 h) with slow agitation. $OD_{280}$ of the supernatant was measured. Assigning the difference in $OD_{280}$ to the amount of protein bound, static capacity was determined as this amount divided by the amount of resin present in the solution.

#### 2.3.6. Particle size distribution measurements

Particle size distribution was measured by Coulter counting. A few drops of resin in suspension were added to 100 ml of 0.9% NaCl solution. A preliminary counting of the solution was performed to ensure that the coincidence factor was below 10%. The final measurement was thus performed, counting more than 60000 particles. A 280 μm i.d. orifice tube was employed for the measurements.

#### 2.3.7. SEM pictures

Imaging was carried out on a FEI Quanta 200 scanning electron microscope at an acceleration voltage of 10 kV or 12.5 kV. The chamber was kept in low vacuum mode at a pressure of 0.45 Torr and a temperature of approximately 21 °C (ambient). The low vacuum mode eliminates charging of the samples and avoids the use of the conventional conductive coating. The secondary electrons from the sample collide with the water vapour in the chamber creating positive ions, which neutralise the charge build-up on the sample surface. For the SEM analysis, the colloidal resins were deposited on a conducting adhesive pad on the sample stub and evaporated as the sample chamber was pumped down.

#### 2.3.8. Binding strength measurements of insulin precursor

Binding strength measurements of insulin precursor were performed in gradient elution mode. (5 cm length × 1 cm i.d.) columns of SP Sepharose BB, SP Toyopearl 550c, and SP Toyopearl 650c were equilibrated with 8 CVs of a 2.5 mmol/kg HCl + 10 mmol/kg citric acid + 42% (w/w) ethanol solution, pH 2.8. 100 μl of a solution comprising 10 mg/ml pure insulin precursor crystals dissolved in 1 mM HCl was applied, and the column was washed with 10 CVs of equilibration solution. Insulin precursor was eluted by a

20 CVs linear gradient from 0 to 1 mol/kg NaCl in equilibration solution. Salt concentration at the retention time of insulin precursor was determined at the peak maximum of the fairly symmetrical peaks.

### *2.3.9. Dynamic capacity determinations of insulin precursor*

Dynamic capacity determinations of insulin precursor from feed-stock and in pure state were performed by frontal analysis experiments on SP Sepharose BB, SP Toyopearl 550c, and SP Toyopearl 650c according to methods similar to those described elsewhere [30]. Changes in the experimental set-up were: pH and conductivity of the loading solution were 2.8 and ∼10 mS/cm, respectively; flow rate of experiments was 2 ml/min; no washing step was applied; and equilibration was performed with 10 CVs of a 2.5 mM HCl + 10 mM citric acid solution, pH 2.8. Break-through of insulin precursor in the feed-stock experiments was determined by analytical RP-HPLC according to the method described elsewhere [30]. The dynamic capacity at 25 and 50% break-through is presented in this study.

## 3. Results and discussion

The general approach of this study is to compare a number of strong cation-exchange resins at similar conditions. The chromatographic resins presented in Table 2 cover a variety of functions and use including capture and purification in a down-stream process. Resins used for a capture step are characterised by having a fairly large particle size and a high binding capacity that may concentrate the target protein by removal of water and avoid clogging of the column by fermentation products at a high flow rate, e.g. SP Sepharose BB, Toyopearl SP 550c, Toyopearl SP 650c, and partly SP Sepharose XL. Resins for down-stream purification steps are typically characterised by having a small particle size with high selectivity, possibly at high pressure operation. This will result in sharper peaks and a higher resolution of the target protein to the related impurity, e.g. Poros 50 HS, Source 30S, and TSKGel SP-5PW-HR20. The ion-exchangers also cover a broad range of commercially available base matrix chemistries including agarose, methacrylate, and polystyrene-divinyl-benzene. The column diameter employed in the experiments is not optimal for large particle size resins, but was used to minimise the protein consumption. The protein load employed in pH dependence, efficiency, and binding strength experiments was low and it is assumed that experiments were performed at linear chromatography conditions.

Experimental results of pH dependence measurements are presented in Fig. 1. Results of aprotinin and lysozyme with isoelectric points above the experimental pH range display the same expected trend of decreasing retention with increasing pH for all resins, however, the degree of change is fairly modest for all resins. For aprotinin in Fig. 1b, all

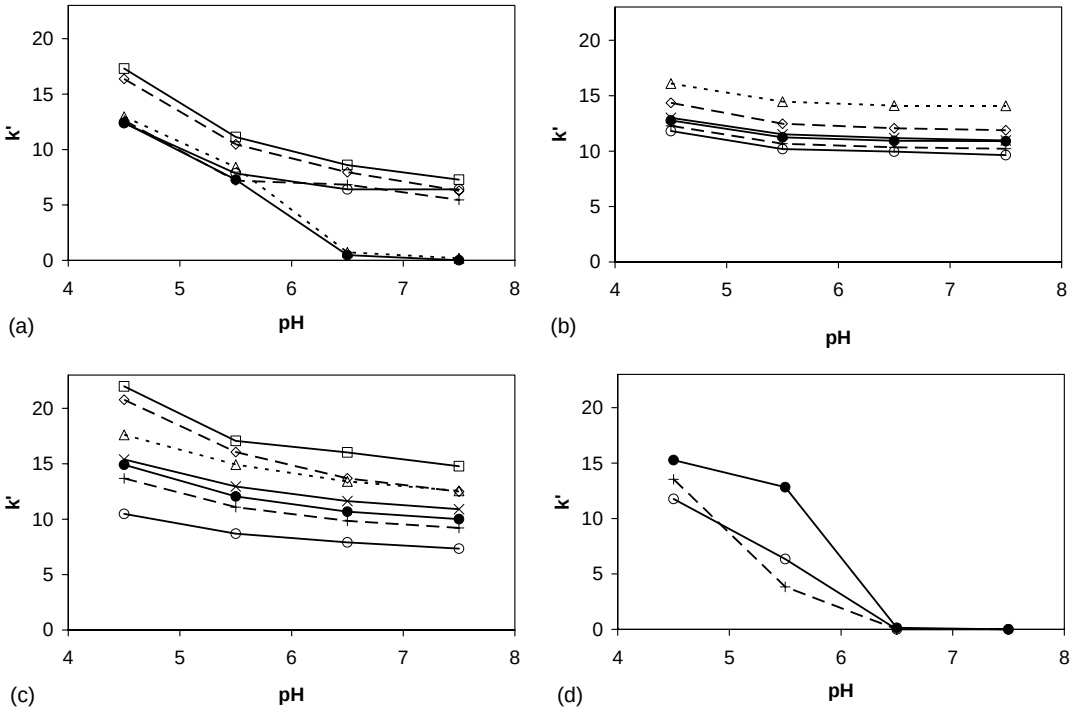


Fig. 1. pH dependence plots ($k'$–pH) of: (a) anti-FVII Mab, (b) aprotinin, (c) lysozyme, and (d) myoglobin on cation-exchange resins. Flow rates are given in Table 2. pH dependence was determined by applying a 20 μl pulse of 1 mg/ml protein solution in 20 CVs linear gradient from 0 to 1 M NaCl in 16.7 mM MES + 16.7 mM HEPES + 16.7 mM sodium acetate buffer through a 10 cm × 0.46 cm or a 10 cm × 0.5 cm column. Symbols are: (×) SP Sepharose XL, (○) SP Sepharose BB, (□) Poros 50 HS, (△) Source 30S, (◇) Toyopearl SP 550c, (+) Toyopearl SP 650c, and (●) TSKGel SP-5PW-HR20.

resins present almost the same retention in the pH range 5.5–7.5, and only at pH 4.5 a slight increase in retention is observed. For lysozyme in Fig. 1c, the same trend is observed, however, some change in retention is observed in the experimental pH range. The largest change in retention for lysozyme is obtained with Toyopearl SP 550c. The order of retention of resins suitable for capture steps is Toyopearl SP 550c > Toyopearl SP 650c > SP Sepharose BB for both proteins. Trends observed for aprotinin and lysozyme in this cation-exchange study are similar to those observed for anion-exchangers with anti-FVII Mab, BSA and lipolase [25,26], however, the dependence on pH are much less pronounced.

Anti-FVII Mab and myoglobin have isoelectric points in the experimental pH range as shown in Table 1. Results of anti-FVII Mab and myoglobin are presented in Fig. 1a and d, respectively, and show the same trend of decreasing retention with increasing pH. For anti-FVII Mab, a rather high retention is observed at pH 7.5 for SP Sepharose BB, Poros 50 HS, Toyopearl SP 550c, and Toyopearl SP650c, which is above the pI of this protein. Though the overall charge of the protein is negative at pH 7.5, the retention experienced could be due to a local area with many positive charges. This finding is analogous to that experienced by the studies with anion-exchangers [25,26]. Essentially, no binding was found for Source 30S and TSKGel SP-5PW-HR20 at pH 6.5 and 7.5. For myoglobin in Fig. 1d, no binding at pH 6.5 and 7.5 where found for the three resins as could be expected with pI of this protein between 7 and 8. Though solutes with pI lower than the pH used should not be suitable for cation-exchange operation, experience from a number of commercial purification processes shows that removal of certain related or unrelated impurities may be performed at such conditions with great advantage.

Data on retention as function of pH is of great importance in process development and optimisation where a change in pH may be necessary to obtain higher buffer strength of the selected buffer system. Fig. 1 could give a hint to how much or if retention would be influenced by such change in pH. Validation issues are always of great importance in the pharmaceutical industry, and these data also give an idea of pH sensitivity of resins when the pH range in a purification process step is settled and challenged. If a selected resin displays too much variation in protein retention as a function of pH, it may be necessary to replace it with a less pH sensitive resin. Finally, data on retention as function of pH is useful for planning of flow-through mode operation and step elution by increase of pH.

Results of the efficiency experiments are presented in Fig. 2 as scaled standard van Deemter plots at unretained conditions. It was assumed that no resin swelling occurred as a function of pH in the range 4.5–7.5. Fig. 2 shows the general trend of higher dependence of the plate height with increasing flow rate of soft resins compared to resins for medium and high-pressure operation. Scatter in the data for some resins is due to difficult and inadequate fitting to the

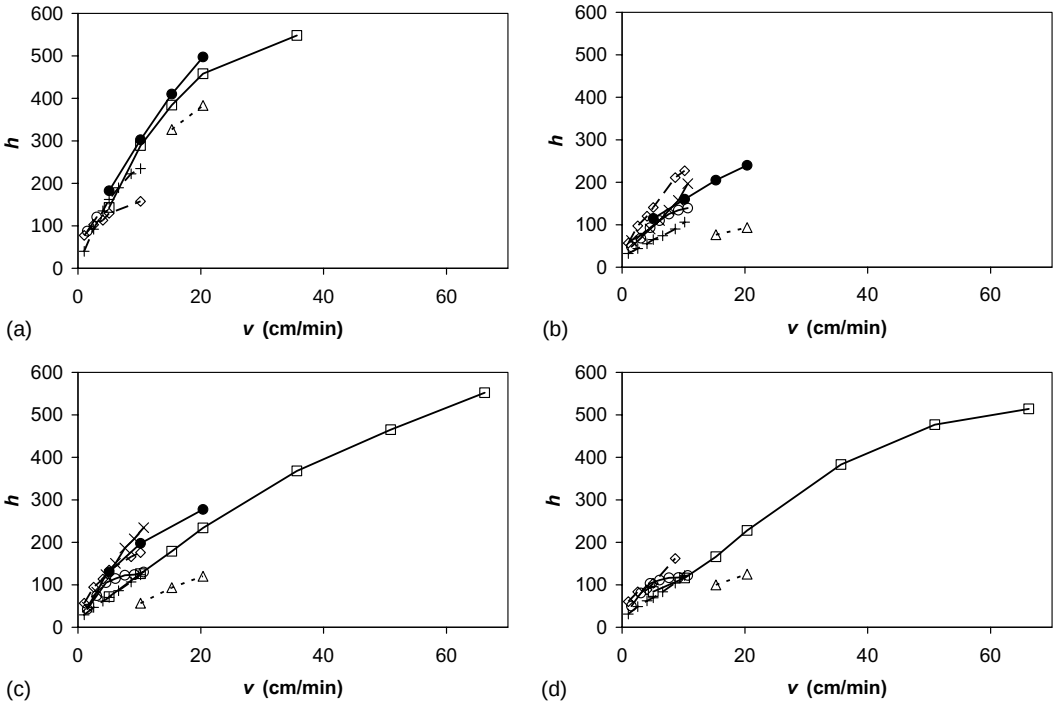


Fig. 2. Efficiency plots ($h$–$v$) of: (a) anti-FVII Mab, (b) aprotinin, (c) Lysozyme, and (d) myoglobin at non-binding conditions. van Deemter curves were determined by applying a 20 μl pulse of 1 mg/ml protein solution in 1 M NaCl in 16.7 mM MES + 16.7 mM HEPES + 16.7 mM sodium acetate buffer at pH 7.5 through a 10 cm × 0.46 cm or a 10 cm × 0.5 cm column. Symbols are: (×) SP Sepharose XL, (○) SP Sepharose BB, (□) Poros 50 HS, (△) Source 30S, (◇) Toyopearl SP 550c, (+) Toyopearl SP 650c, and (●) TSKGel SP-5PW-HR20.

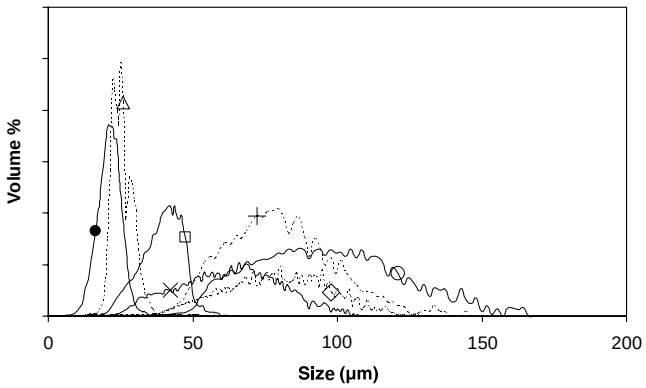


Fig. 3. Particle size distribution (vol.%) of new anion-exchange resins in 0.9% NaCl measured by Coulter counting. Symbols are: (×) SP Sepharose XL, (○) SP Sepharose BB, (□) Poros 50 HS, (△) Source 30S, (◇) Toyopearl SP 550c, (+) Toyopearl SP 650c, and (●) TSKGel SP-5PW-HR20.

EMG function, and because determination of *h* involves calculation with very small numbers which may be associated with some degree of uncertainty. The fairly low absolute values of *h* are a direct result of the EMG function fitting procedure taking the peak tailing fully into account compared to other fitting methods. The vertical position of some resins in Fig. 2 would change if the mean particle size found in this study was used instead of supplier data (see below), however, this was not done but the effect would be most pronounced for SP Sepharose BB. The trend of the curves is as expected. The trend of descending increase of *h* values with increasing flow rate obtained for most resins may be due to emerging compression of the resins. This trend is most distinct for SP Sepharose BB with nominally the largest particle size and probably the softest resin of this study. Toyopearl SP 650c and Poros 50 HS present the same trend for anti-FVII Mab.

Plate height data may be used in process development as an indication of the purification efficiency to be expected for the individual resins at a specified column length and flow rate. For process optimisation and validation, these data will indicate the influence of a change in flow rate for a specific purification step on separation efficiency.

Particle size distribution was measured by Coulter counting for unused resins. Fig. 3 shows the results, and the mean particle size (50%) is presented in Table 2. Distributions in Fig. 3 increase with the mean particle size. The results are in agreement (within 20%) with supplier data for most resins, however, much smaller particles were found for SP Sepharose BB and to some extent for SP Sepharose XL. All results were verified by scanning electron microscopy (see below). The difference in results between these studies and supplier data for Sepharose resins may be due to the slightly different methodologies applied. According to Amersham Biosciences, the reason for the lower value of particle diameter of this study is that our instrument is only calibrated with solid latex particles. For calibration, Amersham Biosciences also take the porosity into consideration, by image analysing a sieved fraction of the sample and Coulter counting the same fraction. The calibration factor obtained thereby compensates for the fact that there is electrolyte solution also inside the particles, since the particles are porous. For solid particles, the calibration factor would be 1, and for Sepharose particles it is around 1.5. This brings the values of SP Sepharose BB for this study and for Amersham Biosciences completely in line.

To verify particle size distribution results found by Coulter counting, size distribution was measured directly on SEM pictures, see Table 2 and Fig. 4. Although this methodology is encumbered with dept due to measurement on a very small and possibly not representative sample, it may give an idea of the validity of size distribution results by Coulter counting. Whether any shrinkage of resins appears due to dehydration during SEM imaging is not known, however, a very good agreement of the mean particle size is obtain in Table 2 by the two independent methods. The size distribution by SEM imaging in Table 2 and by Coulter counting in Fig. 3 is also in good agreement. Upon examination of Fig. 4, the structure and shape of resin particles can be observed. The agarose particles in Fig. 4a and b seem somewhat collapsed in their shape, SP Sepharose XL being most irregular. This is surprising and not in concordance with our previous results obtained with Q Sepharose FF (unpublished results of [26]), and could be due to dehydration of the resins. There are also some clear indications of some of the particles having grown together, especially for SP Sepharose BB. Poros 50 HS, Source 30S, and TSKGel SP-5PW-HR20 in Fig. 4c, d, and g, respectively, are all regular in their shape, and the mono-dispersed nature of Source 30S is clearly observed. The two Toyopearl resins in Fig. 4e and f are very similar in structure as expected. Result on mean particle size for Source 30S is in very good agreement with results obtained by Nash and Chase [6]. Further, results on particle size distribution for Poros 50 HS is in agreement with results obtained by Weaver and Carta [16].

Data on particle size distribution is important when the column filter of industrial columns is selected. If resin particles are smaller than stated or have a different shape than expected, they may clog up the filter leading to increased column backpressure and the risk of damaging column and chromatographic resin. Further, it is important to know the methodology used by suppliers to measure particle size distribution of resins in the selection of column filters if differences or problems arise.

The binding strength is obtained by isocratic runs as presented in Fig. 5. In this study, binding strength is characterised by standard $k'$ versus $I_{\text{Total}}^{-1}$ plots, thus stronger binding will need more salt for elution to occur and thus smaller $I_{\text{Total}}^{-1}$. The strongest binding of test proteins with high isoelectric point, aprotinin and lysozyme in Fig. 5b and c, is obtained for Toyopearl SP 550c, while the resin with the weakest binding is Toyopearl SP 650c. Toyopearl SP 550c and Toyopearl SP 650c have the same base matrix chemistry and should only differ in the pore size distribution,

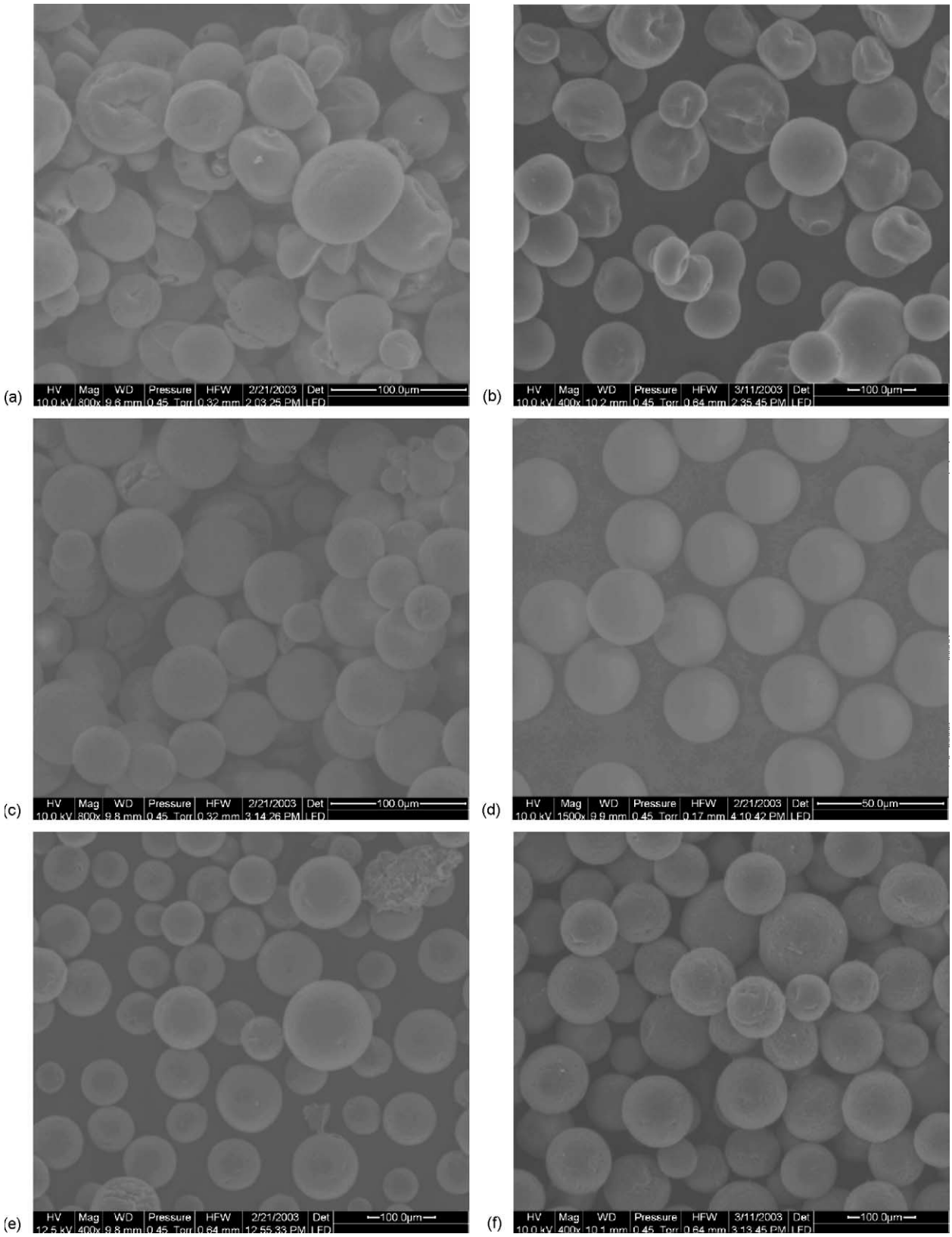


Fig. 4. SEM images of chromatographic resins at different magnification. Scale appears in the separate figures. Resins are: (a) SP Sepharose XL, (b) SP Sepharose BB, (c) Poros 50 HS, (d) Source 30S, (e) Toyopearl SP 550c, (f) Toyopearl SP 650c, and (g) TSKGel SP-5PW-HR20.

(g)

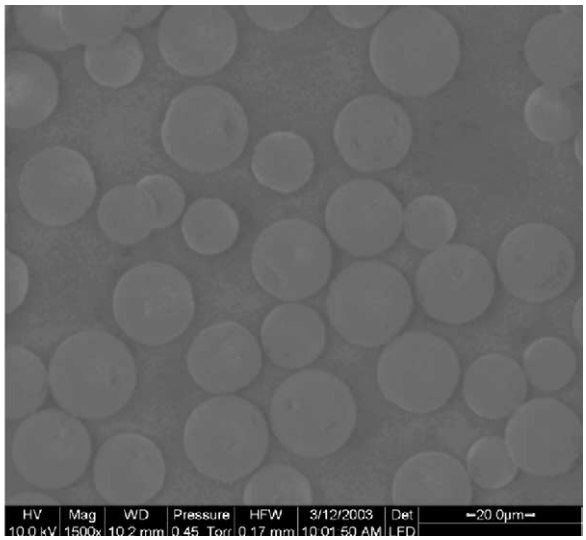


Fig. 4. (*Continued*).

Toyopearl SP 650c having the smallest pores, however, the pore size thus have a very high influence on binding strength. The same trend was observed for anti-FVII Mab and Lipolase on the corresponding strong anion-exchangers, Toyopearl QAE 550c and Toyopearl SuperQ 650s [26]. SP Sepharose XL has the same base matrix chemistry as SP Sepharose BB, and the dextran coating of SP Sepharose XL appears not to have influence on binding strength of lysozyme. For the corresponding strong anion-exchangers, this was the case for some proteins [26]. Poros 50 HS and Source 30S resins both based on polystyrene/DVB also present the same trend as for the corresponding strong anion-exchangers: Poros 50 HS appears to bind at fairly high salt concentration, while Source 30S binds at somewhat lower salt concentrations. Retention obtained on cation-exchangers is higher than on corresponding anion-exchangers [25,26]. This is likely due to the different amino acid composition of the various solutes, and in concordance with general experience from the pharmaceutical industry. The order of retention of resins suitable for capture steps is Toyopearl SP 550c > SP Sepharose BB > Toyopearl SP 650c for both proteins with high isoelectric point. This is in contrast with the findings of the pH dependence study, and is due to different methods for determination of $k'$ and different retention mechanisms applied in the two studies. Significant tailing of peaks in the pH study was also observed in some cases but not accounted for, thus the retention order of binding strength study is assumed to be most correct. For the two test proteins with low isoelectric point, anti-FVII Mab and myoglobin in Fig. 5a and d, similar trends are in general observed as for aprotinin and lysozyme. DePhillips and Lenhoff [4] have also performed

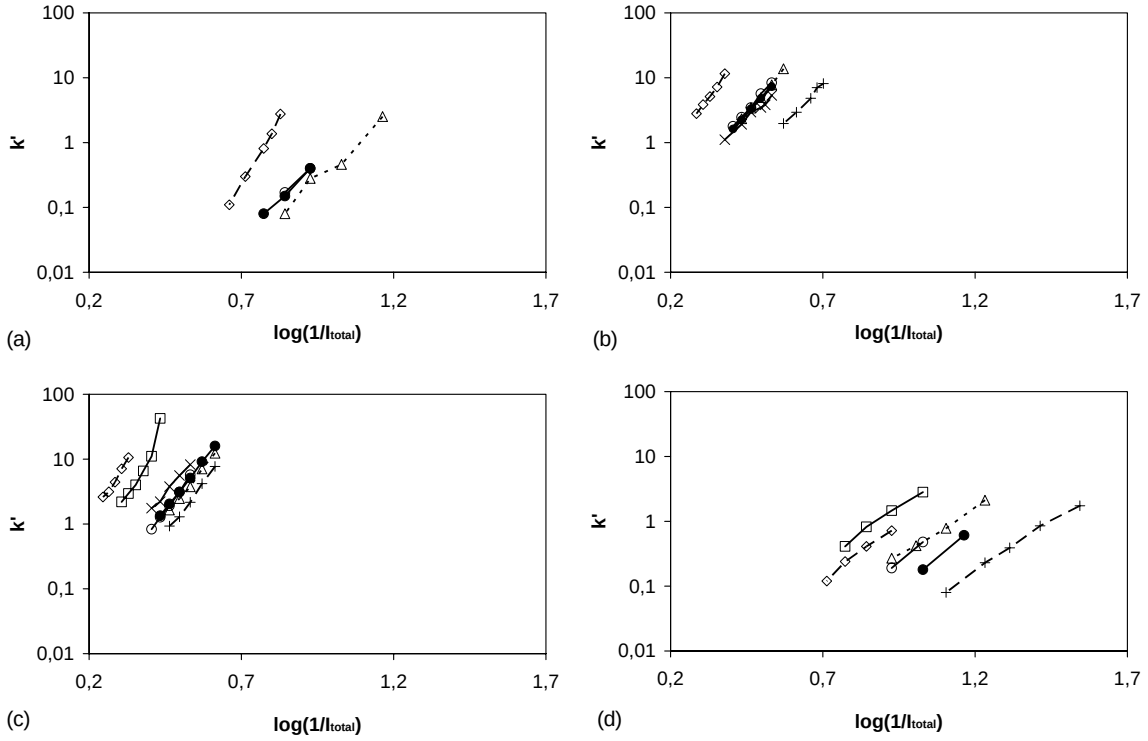


Fig. 5. Binding strength plots ($k'$–$I_{\text{Total}}^{-1}$) at pH 5.5 of: (a) anti-FVII Mab, (b) aprotinin, (c) lysozyme, and (d) myoglobin on cation-exchange resins at approximately 50% of recommended maximum operating flow rate. Actual flow rates are given in Table 2. Binding strength was determined by applying a 20 μl pulse of 1 mg/ml protein solution in 16.7 mM MES + 16.7 mM HEPES + 16.7 mM sodium acetate at various isocratic NaCl concentrations through a 10 cm × 0.46 cm or a 10 cm × 0.5 cm column. Symbols are: (×) SP Sepharose XL, (○) SP Sepharose BB, (□) Poros 50 HS, (△) Source 30S, (◇) Toyopearl SP 550c, (+) Toyopearl SP 650c, and (●) TSKGel SP-5PW-HR20.

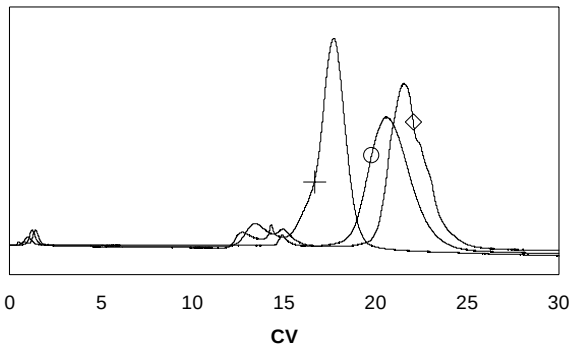


Fig. 6. Retention of insulin precursor in a linear NaCl gradient from 0 to 1 mol/kg over 20 CVs. Solvent system is 2.5 mmol/kg HCl + 10 mmol/kg citric acid (+) 42% (w/w) ethanol solution, pH 2.8. Symbols are: (○) SP Sepharose BB, (◇) Toyopearl SP 550c, and (+) Toyopearl SP 650c.

extensive studies of $\log k'$ as a function of NaCl concentration including measurements with lysozyme on Toyopearl SP 550c, Toyopearl SP 650c, and SP Sepharose FF. Assuming similar properties of SP Sepharose FF and SP Sepharose BB (same resin with different particle size), they found the same order of binding strength of the three resins, with Toyopearl SP 550c being the strongest retaining resin of all.

To test the validity of binding strength tests and suitability of results with model proteins for prediction of comparability of resins, a different protein was tested with the three resins suitable for capture step operation. The protein tested was insulin precursor in an ethanol containing solvent system. Based on the results of model proteins, the following order of resins for binding strength should be assumed for insulin precursor: Toyopearl SP 550c > SP Sepharose BB > Toyopearl SP 650c. Fig. 6 presents the results of binding strength tests with insulin precursor with gradient operation, and the order of resins is as expected by a simple evaluation of retention times. Salt concentration at the retention time of the solute for the three resins is given in Table 4.

Binding strength determination is of great importance for resin selection and optimisation of ion-exchange purification processes. If the target protein binds weakly due to its presence in a loading solution of high conductivity and/or various modifiers, selection of resins for further testing should be among those to the left in the figures. In case of a protein binding strongly to all resins, a resin located to the right in the figures would probably be selected for further testing to minimise salt consumption or to avoid pH changes for elution. In flow-through mode chromatography operation for removal of impurities, the target protein passes through the resin, which retains the impurities preferably at the conditions of the loading sample. For this purpose, resins to the right in the figures may also apply.

Dynamic capacities are determined by frontal analysis of pure proteins, and 10 and 50% break-through data ($Q_{10\%}$ and $Q_{50\%}$) for anti-FVII Mab, aprotinin, and lysozyme are presented in Table 3 with dynamic capacity data for lysozyme obtained by suppliers. A protein concentration of 1 mg/ml

Table 3
Binding capacity of strong cation-exchange resins for 1 mg/ml solutions of anti-FVII Mab, lysozyme, and aprotinin

| Resin | Dynamic capacity $Q$ (anti-FVII Mab) (mg/ml) | | | | Dynamic capacity $Q$ (aprotinin) (mg/ml) | | | | Dynamic capacity $Q$ (lysozyme) (mg/ml) | | | | Dynamic capacity obtained by the suppliers (lysozyme) (mg/ml) | Static capacity (anti-FVII Mab) (mg/ml) | Static capacity (aprotinin) (mg/ml) | Static capacity (lysozyme) (mg/ml) |
|---|---|---|---|---|---|---|---|---|---|---|---|---|---|---|---|---|
| | Low flow rate | | High flow rate | | Low flow rate | | High flow rate | | Low flow rate | | High flow rate | | | | | |
| | $Q_{10\%}$ | $Q_{50\%}$ | $Q_{10\%}$ | $Q_{50\%}$ | $Q_{10\%}$ | $Q_{50\%}$ | $Q_{10\%}$ | $Q_{50\%}$ | $Q_{10\%}$ | $Q_{50\%}$ | $Q_{10\%}$ | $Q_{50\%}$ | | | | |
| SP Sepharose XL | – | – | – | – | 127 | 141 | 125 | 140 | 188 | 210 | 180 | 210 | >160 | – | 182 | 337 |
| SP Sepharose BB | 13 | 29 | 7 | 23 | 96 | 103 | 81 | 94 | 92 | 103 | 47 | 72 | – | – | – | 138 |
| Poros 50 HS | 27 | 38 | 23 | 35 | – | – | – | – | 43 | 59 | 36 | 55 | 55 | 58 | 58 | 63 |
| Source 30S | 1 | 4 | 1 | 4 | 54 | 56 | 53 | 56 | 79 | 82 | 77 | 80 | >80 | 11 | 63 | 76 |
| Toyopearl SP 550c | 39 | 47 | 25 | 38 | 83 | 117 | 67 | 104 | 107 | 124 | 69 | 95 | 80–120 | 67 | 149 | 139 |
| Toyopearl SP 650c | ~0 | ~0.1 | ~0 | ~0.1 | 26 | 29 | 25 | 29 | 29 | 33 | 28 | 33 | 35–55 | – | – | 41 |
| TSKGel SP-5PW-HR20 | – | – | – | – | 20 | 27 | 20 | 27 | 28 | 39 | 28 | 39 | 20–40 | – | 31 | 41 |

Dynamic capacity results are determined at 10 and 50% break-through, $Q_{10\%}$ and $Q_{50\%}$, at flow rates of approximately 25 and 75% of recommended maximum operating flow rate/pressure. Flow rates are presented in Table 2.

Table 4
Binding strength and dynamic binding capacity of strong cation-exchange resins at 2 ml/min of insulin precursor in feed-stock and in pure state

| Resin | Binding strength (mmol/kg NaCl) | Dynamic capacity $Q$ (mg/ml) | | | |
|---|---|---|---|---|---|
| | Pure state | Pure state | | Feed stock | |
| | | $Q_{25\%}$ | $Q_{50\%}$ | $Q_{25\%}$ | $Q_{50\%}$ |
| SP Sepharose BB | 221 | 62 | 88 | 9 | 41 |
| Toyopearl SP 550c | 253 | 101 | 111 | 6 | 31 |
| Toyopearl SP 650c | 157 | 39 | 43 | 4 | 11 |

Binding capacity results are determined at 25 and 50% break-through, $Q_{25\%}$ and $Q_{50\%}$.

was employed as a realistic concentration for many commercial purification processes. Applied flow rates are given in Table 2. The purpose of this study was to monitor the influence of a fairly high and fairly low flow rate on resin performance. The expected trend of slightly higher dynamic capacity for both 10 and 50% break-through at lower flow rate compared to higher flow rate is presented in Table 3 for all proteins. For Toyopearl SP 550c and SP Sepharose BB, capacity was generally much higher at both 10 and 50% break-through at low flow rate compared to high flow rate due to poor mass transfer into resins particles. This is especially distinct for lysozyme. Dynamic capacity flow rate at the high level employed for Source 30S was equal to the general flow rate used to study other parameters due to pressure problems after extensive use. Good agreement was obtained between this study and supplier data for lysozyme, however, for Toyopearl SP 650c there is a small difference in favour of the suppliers. Any discrepancy may be due to a different experimental setup, possibly for Toyopearl SP 650c where the fairly high buffer solution conductivity (50 mM) may be the reason for the lack of protein binding. A significantly higher capacity of SP Sepharose XL with aprotinin and lysozyme is obtained which support supplier data. Results for lysozyme with Source 30S are in very good agreement with results obtained by Nash and Chase [6] although performed with a higher protein concentration of 2 mg/ml, however, results obtained for IgG on the same resin differ by a factor of more than 10. This is likely due to different properties for the two IgGs, as the dynamic capacity of anti-FVII Mab on all cation-exchangers is generally low, as often experienced with IgG. Weaver and Carta [16] found the dynamic capacity (10% break-through) of a 1 mg/ml lysozyme solution at pH 6.5 with 10 mM phosphate buffer on Poros 50 HS to be approximately 70 mg/ml and approximately 40 mg/ml at flow rates corresponding to the low and high flow rate experiments of this study. Thus, these results are in fair agreement though the flow dependence of Poros 50 HS obtained from this study is much lower.

Static capacity results obtained with 1 mg/ml solutions of anti-FVII Mab, aprotinin, and lysozyme are shown in Table 3. Data was not measured for all resins with anti-FVII Mab and aprotinin. Static capacity is regarded to be the maximum possible capacity that can be obtained for a specific resin. By comparison with dynamic capacity data at 10% break-through, an indication of the fraction of the column utilised during preparative operation is obtained. Excluding the result of Source 30S with lysozyme, the fraction utilised at 10% break-through for the low flow rate range from approximately 50 to 80%; lowest for SP Sepharose XL and highest for Toyopearl SP 550c. A high degree of dependence of dynamic capacity on flow rate is obtained for SP Sepharose BB, Toyopearl SP 550c, and to some extent for Poros 50 HS. This indicates that different degree of improved productivity of the resins may be obtained in process development by decreasing flow rate compared to this study. Chang and Lenhoff [13] obtained static capacity results of 121 and 31 mg/ml with Toyopearl SP 550c and Toyopearl SP 650c, respectively, at pH 7 and 0.1 M NaCl for lysozyme. These results are as expected slightly lower due to the higher salt concentration of their experimental setup than results of this study and thus in very good agreement. Levison et al. [3] also measured static capacity for Toyopearl SP 550c, Toyopearl SP 650c, and Poros 50 HS and found 126, 58, and 70 mg/ml, respectively, which is in agreement with the results of this study, though slightly higher for Toyopearl SP 650c and slightly lower for Toyopearl SP 550c. Results for lysozyme with Source 30S are in very good agreement with results obtained by Nash and Chase [6], while results with IgG differ, as was experienced with studies on dynamic capacity. Weaver and Carta [16] found the static capacity of lysozyme on Poros 50 HS to be approximately 150 mg/ml at pH 6.5 with 10 mM phosphate buffer, which is much higher than that of this study and of Levison et al. [3] (at slightly different conditions).

Binding capacity data is very useful for the industry. If two or more resins during process development perform equally well with respect to resolution, flow rate, price, etc., the resin with the highest capacity will be chosen to increase productivity. However, binding capacities of true mixtures such as fermentation broth give a more realistic picture of what to expect in a process development situation [30]. To test the validity of dynamic capacity results of model proteins and their suitability for prediction of resin comparability, insulin precursor in pure state and in real feed-stock were tested with the three resins suitable for capture operation. Based on the results of model proteins, the following order of resins for dynamic binding capacity should be assumed for insulin precursor: Toyopearl SP 550c > SP Sepharose BB > Toyopearl SP 650c. Table 4 presents the results of dynamic capacity. As seen from Table 4, the order of resins for pure

insulin precursor is as expected, however when situated in feed-stock, dynamic capacity is higher for SP Sepharose BB than for Toyopearl SP 550c. The reason could be that competitive binding of various components in the feed-stock are more susceptible to binding on Toyopearl SP 550c than on SP Sepharose BB resulting in the higher insulin precursor capacity for the latter. Though SP Sepharose BB seems to be the best resin for capture of insulin precursor, experimental conditions were not optimised for either resin, and the most important message here is that results for pure proteins may be used only for selection of a few appropriate resins for further testing and optimisation for the specific purpose.

## 4. Conclusion

A comparative study was performed on strong cation-exchangers to investigate the pH dependence, efficiency, binding strength, particle size distribution, static and dynamic capacity, and SEM pictures of the chromatographic resins. A general good agreement was obtained between this study and data obtained by others. The validity of experiments and results with model proteins were tested using a protein, human insulin precursor in pure state and in real feed-stock on Toyopearl SP 550c, SP Sepharose BB, and Toyopearl SP 650c. Results showed good agreement with experiments with model proteins.

Data generated in this study should be used for selection of resins for further testing in process development. However, the data cannot be used to estimate selectivity differences or resolution between target proteins and specific impurities. None of the resins should be regarded as good or poor for chromatographic operation but more or less suitable for a specific purpose, and only testing for the specific application will determine which resin is optimal.

## 5. Nomenclature

| | |
|---|---|
| $A$ | scaling parameter |
| $c_i$ | molar concentration of component $i$ |
| $C/C_0$ | normalised protein concentration |
| CVs | column volumes |
| $E$ | base line level |
| EMG | exponentially modified Gaussian |
| $I_{\text{Total}}$ | total ionic strength |
| $k'$ | retention factor |
| $M_1$ | first moment of the peak curve |
| $M_2$ | second moment of the peak curve |
| $M_{1,\text{S}}$ | first moment of the extra column volume |
| $M_{2,\text{S}}$ | second moment of the extra column volume |
| $M_{1,0}$ | first moment of the unretained protein |
| $M_{2,0}$ | second moment of the unretained protein |
| $\text{OD}_{280}$ | optical density at 280 nm. |
| $v$ | linear flow rate |
| $v_{\text{vol}}$ | volumetric flow rate |
| $Z$ | dummy parameter |
| $z_i$ | ionic charge of component $i$ |
| $\mu$ | Gaussian mean retention time |
| $\sigma$ | symmetrical peak width |
| $\tau$ | asymmetrical peak width |

## Acknowledgements

The supply of Novo Nordisk proteins from Claus Rix Melchiorsen, Birgitte Silau, and Ole Elvang Jensen, and set up of dynamic capacity measurements and EMG data fitting procedures from Ulrik Borgbjerg are gratefully acknowledged. A special acknowledgement to Liv Johansen from Amersham Biosciences for insight in their Coulter counting procedures.

## References

[1] P. DePhillips, A.M. Lenhoff, J. Chromatogr. A 883 (2000) 39.
[2] E. Boschetti, J. Chromatogr. A 658 (1994) 207.
[3] P. Levison, C. Mumford, M. Streater, A. Brandt-Nielsen, N.D. Pathirana, S.E. Badger, J. Chromatogr. A 760 (1997) 151.
[4] P. DePhillips, A.M. Lenhoff, J. Chromatogr. A 933 (2001) 57.
[5] R. Noel, G. Proctor, Predictive Evaluation of Chromatographic Media Performance in Process Scale Production of Antibodies, Poster presentation at Recovery of Biological Products X, Cancun, Mexico, June 2001.
[6] D.C. Nash, H.A. Chase, J. Chromatogr. A 807 (1998) 185.
[7] J. Horvath, E. Boschetti, L. Guerrier, N. Cooke, J. Chromatogr. A 679 (1994) 11.
[8] S. Yamamoto, T. Ishihara, J. Chromatogr. A 852 (1999) 31.
[9] S. Yamamoto, E. Miyagawa, J. Chromatogr. A 852 (1999) 25.
[10] J. Renard, C. Vidal-Madjar, B. Sebille, J. Liq. Chromatogr. 15 (1992) 71.
[11] L. Dunn, M. Abouelezz, L. Cummings, M. Navvab, C. Ordnez, C.J. Siebert, K.W. Talmadge, J. Chromatogr. 548 (1991) 165.
[12] M. McCoy, K. Kalghatgi, F.E. Regnier, N. Afeyan, J. Chromatogr. A 743 (1996) 221.
[13] C. Chang, A.M. Lenhoff, J. Chromatogr. A 827 (1998) 281.
[14] Y.-B. Yang, K. Harrison, J. Kindsvater, J. Chromatogr. A 723 (1996) 1.
[15] M. Weitzhandler, D. Farnan, J. Horvath, J.S. Rohrer, R.W. Slingsby, N. Avdalovic, C. Pohl, J. Chromatogr. A 828 (1998) 365.
[16] L.E. Weaver, G. Carta, Biotechnol. Prog. 12 (1996) 342.
[17] Y. Hu, P.W. Carr, Anal. Chem. 70 (1998) 1934.
[18] M.A. Hashim, K.-H. Chu, P.-S. Tsan, J. Chem. Technol. Biotechnol. 62 (1995) 253.
[19] R. Hahn, P.M. Schulz, C. Schaupp, A. Jungbauer, J. Chromatogr. A 795 (1998) 277.
[20] C.M. Roth, K.K. Unger, A.M. Lenhoff, J. Chromatogr. A 726 (1996) 45.
[21] F. Fang, M.-I. Aguilar, M.T.W. Hearn, J. Chromatogr. A 729 (1996) 67.
[22] C.B. Mazza, S.M. Cramer, J. Liq. Chromatogr. Relat. Technol. 22 (1999) 1733.
[23] K. Hamaker, S.-L. Rau, R. Hendrickson, J. Liu, C.M. Ladisch, M.R. Ladisch, Ind. Eng. Chem. Res. 38 (1999) 865.
[24] V. Natarajan, S.M. Cramer, J. Chromatogr. A 876 (2001) 63.
[25] A. Staby, I.H. Jensen, I. Mollerup, J. Chromatogr. A 897 (2000) 99.

[26] A. Staby, I.H. Jensen, J. Chromatogr. A 908 (2001) 149.
[27] L. Thim, S. Bjørn, M. Christensen, E.M. Nicolaisen, T. Lund-Hansen, A.H. Pedersen, U. Hedner, Biochemistry 27 (1988) 7785.
[28] H. Fritz, G. Wunderer, Arzneim.-Forsch./Drug Res. 33 (4) (1983) 479.
[29] E. Grushka, Anal. Chem. 44 (1972) 1733.
[30] A. Staby, N. Johansen, H. Wahlstrøm, I. Mollerup, J. Chromatogr. A 827 (1998) 311.
[31] I. Mollerup, S.W. Jensen, P. Larsen, O. Schou, L. Snel, Insulin, purification, in: M.C. Flickinger, S.W. Drew (Eds.), The Encyclopedia of Bioprocess Technology: Fermentation, Biocatalysis and Bioseparation, Wiley, NY, 1999.